Journal of Thermal Analysis and Calorimetry, Vol. 91 (2008) 3, 749–757

ISOTHERMAL CRYSTALLIZATION OF LAYERED SILICATE/STARCH-POLYCAPROLACTONE BLEND NANOCOMPOSITES

C. J. Perez, A. Vázquez and V. A. Alvarez[*]

Research Institute of Material Science and Technology (INTEMA), – National University of Mar del Plata (UNMdP)
Av. Juan B. Justo 4302, 7600 Mar del Plata, Argentina

The isothermal crystallization behavior of layered silicate/starch-polycaprolactone blend nanocomposites was studied by means of differential scanning calorimetry (DSC) measurements. The theoretical melting point was higher for the matrix than for nanocomposites. At low clay concentration, the induction time decreased and the overall crystallization rate increased acting as nucleating agent whereas at higher concentrations became retardants. Classical Avrami equation was used to analyze the crystallization kinetic of these materials. *n* values suggested that clay not only affected the crystallization rate but also influenced the mechanism of crystals growth. An Arrhenius type equation was used for the rate constant (*k*). Models correctly reproduced the experimental data.

Keywords: *Avrami equation, biodegradable polymers, clays, crystallization, modeling, nanocomposites*

Introduction

Biodegradable polymers are growing mainly due to ecological reasons [1–3]. Commercial starch based blends are very useful for the management of post-consumer waste and are used especially for packaging industry [4–6].

Polymeric materials have been filled with several inorganic synthetic and/or natural compounds in order to increase several properties (especially mechanical and impact properties) and decrease others (such as gas permeability) [7–16].

In the case of crystalline polymers, mechanical and physical properties are strongly dependent on the crystal structure and morphology that are related with the crystallization degree. Cyras *et al.* [4] have studied the effect of natural fibres (sisal) on the crystallization behaviour of MaterBi-Z (polycaprolactone/starch blend). They have found that the Avrami exponent, *n*, was close to 2 for the matrix and that this exponent remained constant when sisal fibres were incorporated up to 30 mass%. On the other hand, they demonstrated that for a given crystallization temperature, the induction time and the half-time of crystallization increased with fibers incorporation (30 mass%). An increase on the half-time of crystallization is related with a decrease on the crystallization rate. Both activation energies (for induction time and for the rate constant) slightly increased when fibres were added.

In the case of nanocomposites, investigation of the early stages of crystallization is of particular interest, because of the possible role of clay platelets and tactoids in crystal nucleation. It has been studied that clay particulates greatly affects the crystallization behaviour and morphology of polymer matrix. In several cases, heterogeneous nucleation was observed [15, 17, 18].

Nanoparticles can either increase or decrease the global crystallization rate of a semicrystalline polymer: Fornes *et al.* [19] have shown that high clay concentrations reduce the rate of crystallization in the case of Nylon 6/MMT nanocomposites. Similar effects have been observed for nanocomposites in other matrices like PCL systems. Di Maio *et al.* [18] have studied the case of PCL (polycaprolactone)/MMT. They showed that the addition of 0.1% of nanoclay resulted in a reduction of the crystallization half-time to less than 1/2 of that of the pure matrix. The highest crystallization rate was achieved with 0.4% of clay. At higher nanoclay concentration, the crystallization rate started to decrease. Furthermore, besides the influence on nucleation, a retarding effect of the silicate layers on the crystal growth of polymer matrices has been found [19–21]. In the crystallization of extruded PA-6 (polyamide-6)/MMT nanocomposites, the overall crystallization rate decreases with increasing silicate layer content at the highest silicate layer contents, or even over the full silicate layer content range [19].

Another important effect of clay incorporation is the change on the crystallinity degree which is strongly related with final mechanical properties. Strawhecker *et al.* [22] have shown for PEO that the enthalpy of melting (measured by DSC), showed no strong effect of the silicate loading and/or the crystal-

* Author for correspondence: alvarezvera@fi.mdp.edu.ar

1388–6150/$20.00
© 2008 Akadémiai Kiadó, Budapest
Akadémiai Kiadó, Budapest, Hungary
Springer, Dordrecht, The Netherlands

lization temperature (T_c) on the final crystallinity but that the addition of MMT decreased the of the neat polymer for all cooling rates used, suggesting that the MMT hinders the PEO crystallization. On the other hand, the crystal morphology was strongly altered by the MMT presence, resulting in more, smaller, and nonisotropic crystallites. Nevertheless, Plutta *et al.* [23] have found a decrease on the crystallinity degree in the case of polylactide (PLA) in PLA-clay nanocomposites.

Non-isothermal crystallization of MaterBi-Z and its nanocomposites with different clay contents (0, 2.5 and 5 mass%) was previously studied. Clay without modification was used and the experimental data showed that clay can be act both as nucleating or retarding agent depending on the clay content. Kinetic parameters obtained by using a non-linear regression method, i.e, Kamal's model and Dietz's modification, were able to describe the non-isothermal crystallization behavior of the studied materials [24]. The method for fitting the experimental results is related with a general model behavior and for understanding the mechanism of crystallization it is necessary to obtain the Avrami parameters as well as in order to compare the crystallization parameters with other polymer under isothermal crystallization method.

The aim of this work was to study the mechanism of crystallization of layered silicate/starch-polycaprolactone blend nanocomposites by means of the isothermal crystallization mode. The effect of the clay concentration and clay type by application of theoretical models will also be analyzed.

Theoretical background

During crystallization, the developed heat yields exothermic peaks in DSC, which represent the plot of rate of heat evolution; dQ/dt; *vs.* temperature or time. When the DSC operates isothermally, the crystallization heat can be obtained by measuring the area under the thermogram peak [25]. The relative degree of crystallinity (α) is obtained from the area of the exothermic peak in DSC isothermal crystallization analysis at a crystallization time (t) divided by the total area under the exothermic peak.

$$\alpha = \frac{\int_0^t \frac{dH}{dt} dt}{\int_0^\infty \frac{dH}{dt} dt} = \frac{\Delta H_t}{\Delta H_0} \quad (1)$$

where the numerator is the heat (ΔH_t) generated at time t and the denominator is the total heat (ΔH_0) generated up to the complete crystallization.

Polymeric matrices crystallization kinetics under isothermal conditions can be model by the Avrami equation in which the rate constant can be usually expressed by an Arrhenius-type relationship with temperature [26].

Experimental

Materials

MaterBi-Z (a commercial Starch/Polycaprolactone blend) kindly supplied by Novamont, Novara, Italy was used as a matrix. Three different clays were used: one unmodified and two modified. The organoclays are prepared by modification of natural montmorillonite clays with different quaternary ammonium salts. These clays were purchased from Southern Clay Products Inc., USA, under the commercial name of:

- Cloisite Na^+ (unmodified montmorillonite),
- Cloisite 30B® (modified with

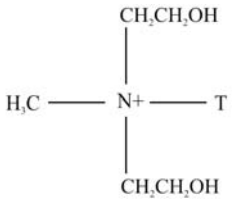

concentration: 90 meq/100 g of clay) and
- Cloisite 10A® (modified with

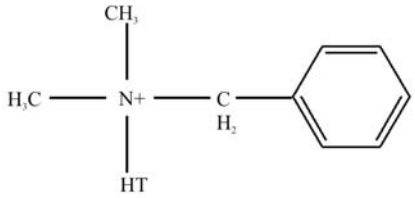

concentration: 125 meq/100 g of clay).

Composite preparation

An intensive Brabender type mixer with two counter-rotating roller rotors was used for the preparation of the MaterBi-Z/organoclay nanocomposites with different compositions. The processing temperature was set at 100ºC. The rotating speed of the rotor and the mixing time were 150 rpm and 10 minutes. The concentration of clay ranged from 0.5 to 5 mass% based on the polymer.

After mixing, the samples were compression molded between the hot plates of a hydraulic press for 10 min at 100°C. Initially a low pressure was applied to mold the polymer. The thickness of the samples was between 0.3–0.5 mm.

It was demonstrated in a previous paper [27] by X-ray diffraction (XRD) that the most of the clays are intercalated within the polymeric chains giving intercalated nanocomposites.

Methods

A Perkin Elmer 7 DSC (Differential Scanning Calorimeter) was used for the study. Samples of about 10 mg were accurately weighted. All DSC analyses were performed under nitrogen atmosphere. A first run was done from 25 to 100°C at 20°C min^{-1}. Then the samples were melted for 10 min at 100°C, cooled to the crystallization temperature at 40°C min^{-1}, and maintained at the crystallization temperature 30 min to allow complete crystallization. The materials were crystallized in the temperature range of 36–44°C. Then the materials were heated from the crystallization temperature to 100ºC at 10°C min^{-1} to melt formed crystals at the crystallization temperature and to find the melting temperature of each material.

Results and discussion

Figure 1 shows the heating run after isothermal crystallization at different temperature for the pure matrix (MaterBi-Z). Melting temperature increased with the increment in the isothermal crystallization temperature. This behavior was also exhibited in the other studied materials i.e. in the nanocomposites and this occurs because chains mobility increases when crystallization temperature increases and that allows the formation of higher crystals and, so that, to a higher melting temperatures. When the crystallization temperature is lower, higher number of smaller size crystals is formed [28].

From ΔH_m of the nanocomposites it is possible to determine a relative degree of crystallinity (with respect to that of the neat matrix). The obtained values are summarized on Table 1. A decrease on the crystallinity degree with clay incorporation can be observed. A similar decreasing trend in crystallization ability of polylactide (PLA) in PLA-clay nanocomposites was observed by Pluta *et al.* [23]. Relatively higher

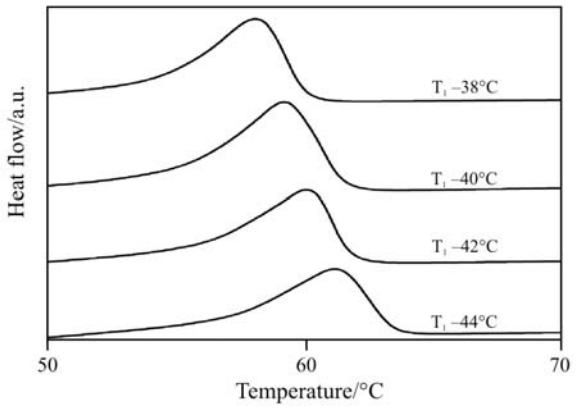

Fig. 1 Dynamic DSC runs for MaterBi-Z after isothermal crystallization at different temperatures

concentrations of organo-clays hinder the polymer chain mobility and effective diffusion of chains to the growing fronts of crystallites is impeded. The limited crystal growth produces crystallites with reduced grain size and lowers the degree of crystallinity. The decrease in crystallinity may further be attributed to the polymer–clay interactions [29].

The thermodynamic melting point (T_m^0) can be determined by Hoffman–Weeks method, extrapolating the experimental points of plot $T_m=f(T_c)$ to the intercept with the plot $T_m=T_c$ [30]. These plots of DSC data are reported on Fig. 2. For all studied materials, the experimental data displayed a good linear regression for the use of this equation. T_m^0 values obtained by the previos method are also summarized on Table 1. Nevertheless the clay content and clay type their addition to MaterBi-Z matrix produced a decrease on the theoretical melting temperature (T_m^0). This phenomenon could probably be related to the presence of more heterogeneous nucleation that reduce the perfection of MaterBi-Z crystallite in the nanocomposite. Similar results were found by Wu *et al.* in the case of Poly(ethylene 2,6-naphthalate)/layered silicate nanocomposites [31].

Nucleation process

The induction time, which is defined as the time needed for the formation of the equilibrium nucleus with critical

Table 1 Theoretical melting point and relative degree of crystallinity for MaterBi-Z matrix and nanocomposites

Clay/mass%	MMT (Montmorillonite Na^+)		C30B (Closite 30B)		C10A (Closite 10A)	
	T_m^0/°C	$x_{c\ rel.}$/%	T_m^0/°C	$x_{c\ rel.}$/%	T_m^0/°C	$x_{c\ rel.}$/%
0.0	71.8	100.0	71.8	100.0	71.8	100.0
0.5	69.0	98.2	64.4	96.7	67.3	100.0
1.0	66.6	99.3	63.1	94.4	63.3	100.0
2.5	67.1	97.4	70.8	94.9	67.8	96.0
5.0	69.5	98.8	68.5	89.0	70.1	98.8

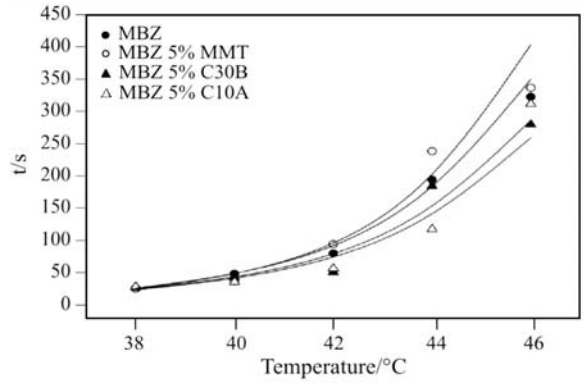

Fig. 2 Hoffman–Weeks analysis. Melting point T_m as a function of the crystallization temperature, T_c for MaterBi-Z matrix and nanocomposites with 5 mass% of clay

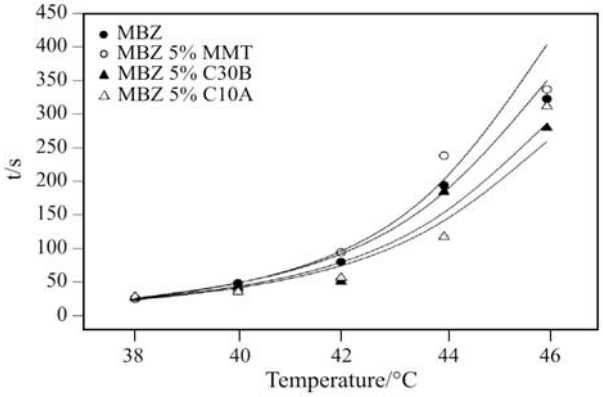

Fig. 3 Induction time as a function of crystallization temperature for MaterBi-Z matrix and nanocomposites with 5 mass% of clay

dimensions at a given T [32], was determined for all the samples. This parameter may be considered as the most suitable macroscopic parameter representative of nucleation process in calorimetric experiments [33] and can be related with temperature. Some of the studied relationships are the following:

$$t_i = K_{ti} \exp\left(\frac{E_{ti}}{R\Delta T}\right) \quad (2)$$

$$t_i = A\Delta T^{-b} \quad (3)$$

where K_{ti} is the preexponential factor, E_{ti} is the activation energy A and b are constants and ($\Delta T = T_m^0 - T_c$).

Figure 3 shows the relationship between the induction time and the crystallization temperature for MaterBi-Z and the nanocomposites with different clay contents. Nevertheless the clay and contents used, induction time increases when crystallization temperature increases; this is due to the decrease on the undercooling which is driving force for crystallization process. The induction time decreased with the addition of unmodified or modified clays. This implies that, due to the high interfacial energy differences between MaterBi-Z and the clays, less time is needed for MaterBi-Z spherulites to heterogeneously nucleate so, they acts as nucleating agent. Krikorian *et al.* [34] have observed a similar tendency for PLLA (poly(L-lactide))/clay nanocomposites.

K_{ti} and E_{ti} values were obtained from Eq. (4) by plotting $\ln t_i$ *vs.* $1/(T_m^0 - T_c)$. The results of this approach are shown on Table 2. The linear dependence between $\ln t_i$ and $1/(T_m^0 - T_c)$ is an indication that there were not morphological changes during crystallization (for selected crystallization temperatures). Activation energy became lower when clay was incorporated (0.5–1 mass%) and then increased. In a similar way, the pre-exponential factor increased with low clay contents and then decreased. Both factors correspond with the fact that induction time decreased when clay were incorporated but then increased.

Growth

The DSC exothermic peak is related with crystal growth. Figures 4 (a–d) shows crystallization peaks for MaterBi-Z and 5 mass% clay nanocomposites and the used crystallization temperatures. Time was scaled by the induction time of each material and temperature. As it was expected, the crystallization rate decreased as the crystallization temperature increased nevertheless the material. That is due to the lower undercooling degree, i.e. the lower crystallization driving force. Curves were transformed in degree of crystallinity *vs.* time curves as is shown on Figure 5 for crystallization at 40°C. From this figure it is clear that low clay

Table 2 Activation energy and pre-exponential factor for MaterBi-Z matrix and nanocomposites

Clay/mass%	MMT		C30B		C10A	
	K_{ti}/s	E_{ti}/kJ mol^{-1}	K_{ti}/s	E_{ti}/kJ mol^{-1}	K_{ti}/s	E_{ti}/kJ mol^{-1}
0.0	$1.6\cdot10^{-2}$	1.99	$1.6\cdot10^{-2}$	1.99	$1.6\cdot10^{-2}$	1.99
0.5	$1.4\cdot10^{-1}$	1.34	$1.3\cdot10^{-1}$	1.31	$6.9\cdot10^{-2}$	1.07
1.0	$2.2\cdot10^{-3}$	1.34	$3.4\cdot10^{-2}$	0.94	$3.6\cdot10^{-2}$	0.91
2.5	$1.5\cdot10^{-3}$	2.22	$3.5\cdot10^{-3}$	2.15	$1.3\cdot10^{-3}$	2.57
5.0	$4.9\cdot10^{-3}$	2.22	$1.6\cdot10^{-2}$	2.04	$1.0\cdot10^{-2}$	1.84

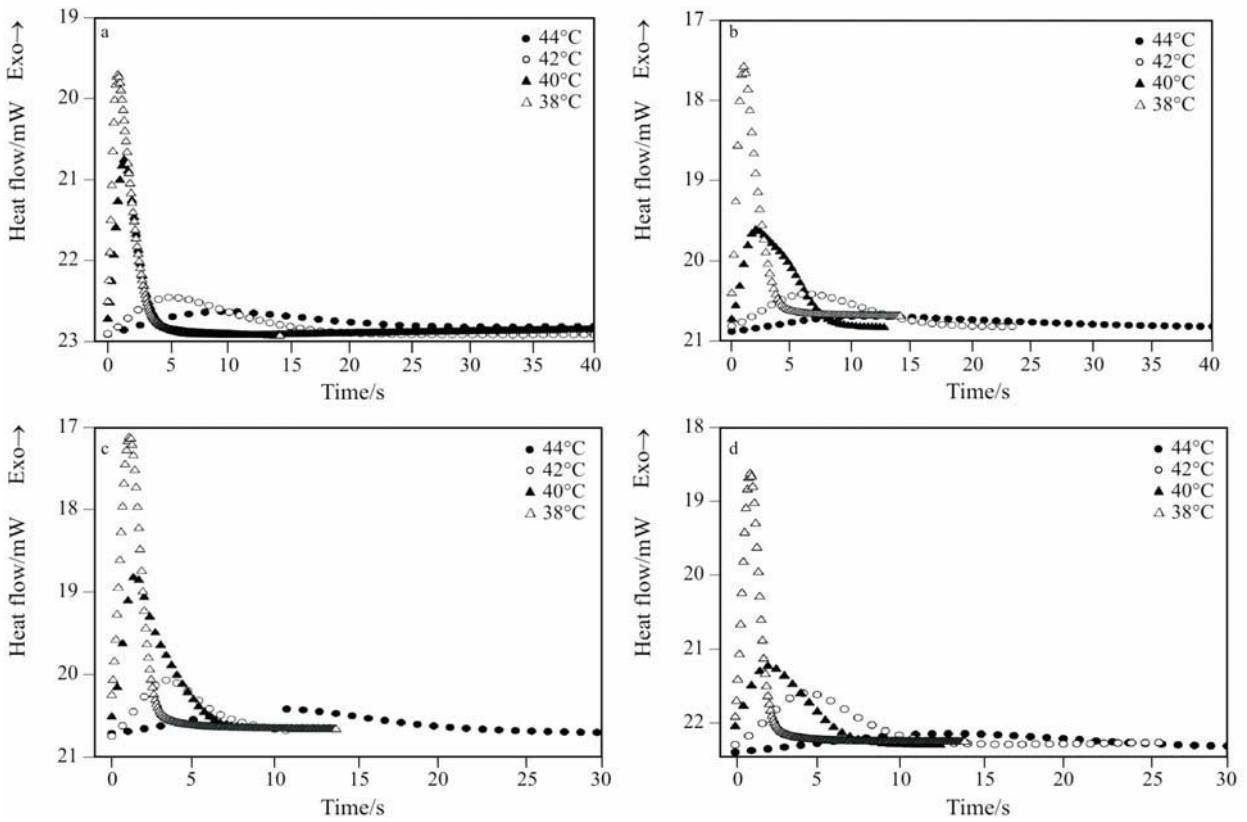

Fig. 4 DSC crystallization exothermic peaks for: a – MaterBi-Z, b – MaterBi-Z 5 mass% MMT, c – MaterBi-Z 5 mass% C30B, d – MaterBi-Z 5 mass% C10A at crystallization several temperatures

concentrations (0.5–1 mass%) accelerate the crystallization process whereas higher clay contents slow down it.

The parameters of Avrami equation were obtained by using a typical non-linear Leberverg–Marquard regression method in the Origin software. Table 3 summarized the obtained values. Crystallization half-time (defined as the time necessary to reach 50% of the total polymer crystallization, after the induction period). For a given kind of material, the crystallization half-time increases following the increase in the crystallization temperature indicating a decrease on the overall crystallization rate which is a common feature observed for semycristalline polymers.

Overall crystallization rate (consider as $1/t_{1/2}$) for a crystallization temperature of 40°C is shown on Figure 6. From this figure it is clear that when clay is incorporated to the neat matrix, the rate of crystallization

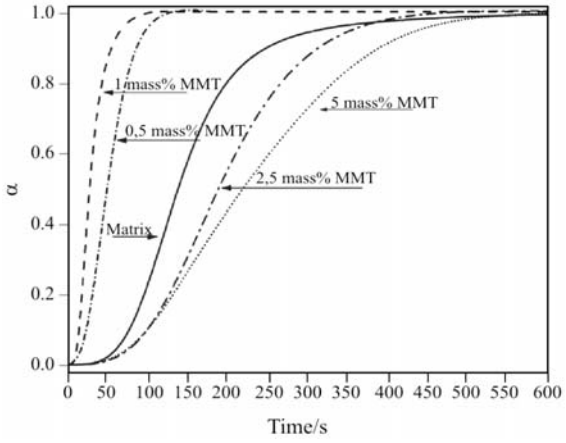

Fig. 5 Relative degree of crystallinity as a function of crystallization time at 40°C for matrix and nanocomposites with 0.5, 1, 2.5 and 5 mass% of MMT

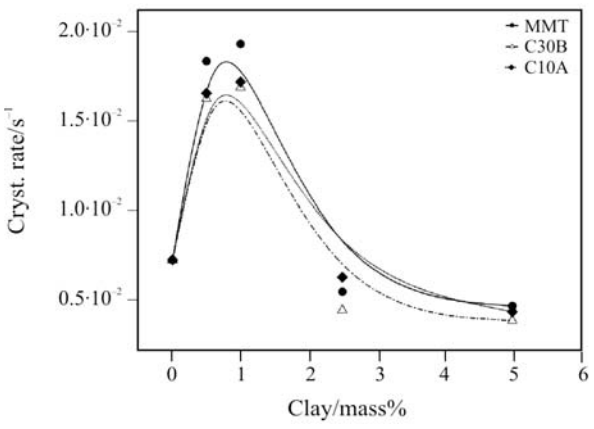

Fig. 6 Overall crystallization rate as a function of clay content for different clays

Table 3 Avrami exponent, n and half crystallization-time $t_{1/2}$ for MaterBi-Z matrix and nanocomposites

Temperature/°C	36		38		40		42		44	
	n	$t_{1/2}$(s)	n	$t_{1/2}$(s)	n	$t_{1/2}$(s)	n	$t_{1/2}$(s)	n	$t_{1/2}$(s)
Matrix	2.38	23.2	2.04	90.7	2.37	141.7	2.08	484.6	2.13	872.0
MaterBi-Z 0.5 mass% MMT	2.23	23.0	2.18	48.0	2.08	102.0	2.77	209.04	2.15	422.2
MaterBi-Z 1.0 mass% MMT	2.21	15.2	1.90	26.8	2.05	52.2	2.37	118.2	2.48	250.8
MaterBi-Z 2.5 mass% MMT	1.80	44.8	2.35	96.9	2.53	190.0	2.89	459.8	2.74	1048.6
MaterBi-Z 5.0 mass% MMT	2.54	46.6	2.06	102.9	2.11	223.8	2.59	552.6	2.44	1287.7
MaterBi-Z 0.5 mass% C10A	2.21	18.5	2.69	24.0	2.69	58.1	2.66	138.2	2.36	262.9
MaterBi-Z 1.0 mass% C10A	2.30	13.2	2.77	29.1	3.13	54.8	3.47	119.9	3.24	257.7
MaterBi-Z 2.5 mass% C10A	2.12	37.3	2.11	85.5	2.52	164.3	2.65	398.5	2.29	1019.8
MaterBi-Z 5.0 mass% C10A	2.41	44.6	2.74	89.5	2.50	241.7	2.71	439.8	3.10	1169.2
MaterBi-Z 0.5 mass% C30B	2.31	23.0	2.11	62.2	2.16	101.1	2.27	235.9	2.30	572.4
MaterBi-Z 1.0 mass% C30B	2.05	18.5	1.99	28.1	2.19	59.8	2.23	137.1	2.99	347.5
MaterBi-Z 2.5 mass% C30B	2.30	39.4	2.53	87.4	2.31	108.7	3.13	238.5	2.92	824.5
MaterBi-Z 5.0 mass% C30B	2.84	38.1	2.87	106.6	2.24	176.9	2.60	267.7	3.09	975.4

increases but with the raise on the clay content a decreasing trend can be observed. Similar results were obtained for all studied temperatures. As it was previously showed by Fornes *et al.* [19] very small amounts of clay dramatically increase the rate of crystallization; however, high clay concentrations reduce the rate of crystallization. The clay particles serve as additional nucleation sites, however high clay contents (higher than 2%) clearly retard the growth process. At low concentration of clay, the distance between disperse platelets is large, so it is relatively easy for the additional nucleation sites to incorporate surrounding polymer. However, at high concentrations of clay, diffusion of polymer chains to the growing crystallite is hindered. The combination of a larger number of nucleation sites and limited crystal growth is expected to produce crystals of fine grain size. So, at low filler concentration interfaces acts as heterogeneous nucleating sites, hence increasing nucleating rate and, therefore, the crystallization kinetics. At higher filler content, diffusion of the polymer chains is hindered and the overall crystallization rate is reduced [24]. Similar results were found by Di Maio *et al.* [18].

The Avrami exponent (n) value depends on two factors: the nucleation mechanism and the geometry of crystal growth. On the other hand, the constant k includes nucleation parameters as well as growth-rate parameters. The average value of the Avrami exponent was close to 2 for the matrix; this value can be interpreted as two dimensional crystal growth with a linear growth rate and the crystal nucleating athermally [35]. The athermal nucleation implies that there is no contribution from nucleation rate to the activation energy [36]. For the nanocomposites, the Avrami exponent values were higher and closer to 3, especially in the case of Cloisite 10A. This result should possible be related with the three-dimensional growth. In the ideal case, n=3 indicates spherical growth while n=2 indicates circular disk shape growth.

In order to compare the values of rate constant (k), an average n value (2.45) was used. Values obtained at 40°C are resumed on Fig. 7. A clear increasing tendency on clay content for low clay concentrations was observed. At higher clay concentrations the trend is upturned. These results are consistent with the previous ones.

ΔT constitutes the driving force of crystallization and indicates that the substantial meaning of the term is to account for the decrease in the overall rate when temperature approaches the thermodynamic melting point; i.e., k decreases with the increase on the crystallization temperature. By using the Arrhenius equation the rate constant can be modeled by using both, linear (by applying logarithm to both sides of Eq. (3)) or non-linear regressions.

Figures 8 a and b show the linear and non-linear regressions for MaterBi-Z and composites with 1 and 5 mass% of different clays. In Fig. 8a almost linear relationships were observed for the matrix and

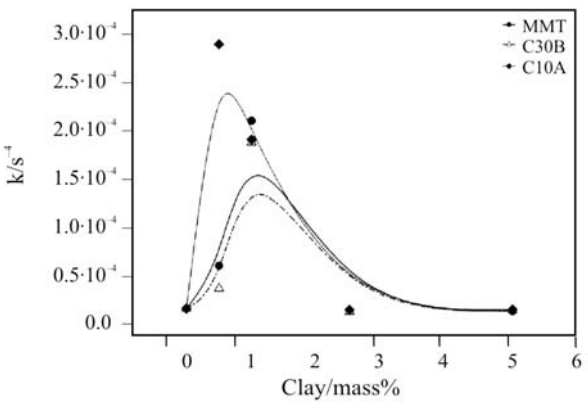

Fig. 7 Rate constant k at 40°C as a function of clay content for different clays

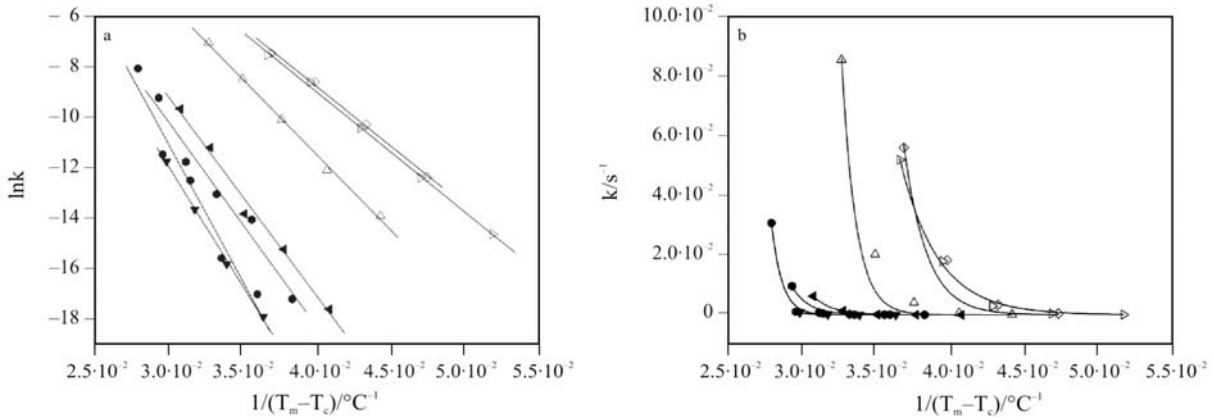

Fig. 8 a – Plot of ln k *vs.* $1/(T_m^0 - T_c)$ and b – k *vs.* $1/(T_m^0 - T_c)$ for matrix and nanocomposites with 1 and 5 mass% of different clays. ● – MBZ, △ – MBZ 1% MMT, ▲ – MBZ 5% MMT, ◇ – MBZ 1% C10A, ◆ – MBZ 5% C10A, □ – MBZ 1% C3OB, ■ – MBZ 1% C30B

nanocomposites with different clay contents. From this plot is possible to obtain pre-exponential factors and activation energies (Ea) for used materials. The results of this regression are reported on Table 4a. Both parameters, the activation energy and the pre-exponential factor, decreased with clay incorporation and, so that, the analysis is quite complicated. By using the non-linear analysis it is possible to fix one of the parameters and to calculate the other one in order to fit the experimental data. The results for this approximation for a constant pre-exponential factor ($1.9 \cdot 10^9$ i.e. the value obtained for the neat matrix) are displayed on Table 4b. These results are more useful in order to analyze the effect of clay on the crystallization process of Mater Bi-Z matrix: the addition of low quantities of layered silicate into the

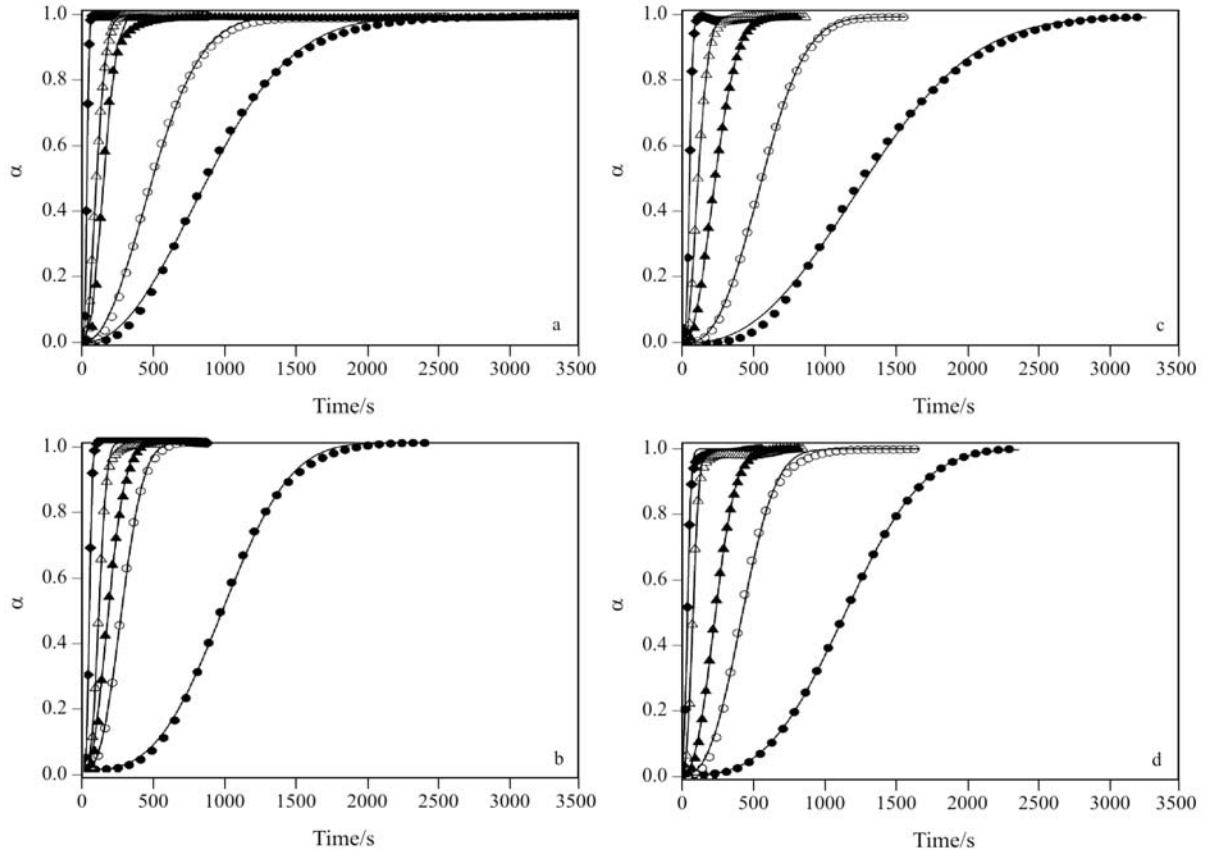

Fig. 9 Degree of crystallinity as a function of time for : a – MaterBi-Z, b – MaterBi-Z 5 mass% MMT, c – MaterBi-Z 5 mass% C30B and d – MaterBi-Z 5 mass% C10A. Lines represent model prediction. T_c: ● – 35, ○ – 38, ◆ – 40, △ – 42 and ▲ – 44°C

Table 4a Results of linear regression for Arrhenius equation for MaterBi-Z and nanocomposites

Clay/mass%	MMT		C30B		C10A	
	$k_0/s^{-2.45}$	E_a/kJ mol^{-1}	$k_0/s^{-2.45}$	E_a/kJ mol^{-1}	$k_0/s^{-2.45}$	E_a/kJ mol^{-1}
0.0	$1.9\cdot10^{9}$	9.0	$1.9\cdot10^{9}$	9.0	$1.9\cdot10^{9}$	9.0
0.5	$1.3\cdot10^{6}$	6.2	$4.8\cdot10^{5}$	5.2	$1.3\cdot10^{5}$	4.4
1.0	$2.5\cdot10^{5}$	5.0	$2.1\cdot10^{4}$	4.0	$2.3\cdot10^{4}$	3.9
2.5	$2.0\cdot10^{6}$	6.3	$1.7\cdot10^{8}$	7.6	$7.5\cdot10^{8}$	8.6
5.0	$1.4\cdot10^{7}$	7.9	$1.3\cdot10^{6}$	6.8	$1.9\cdot10^{6}$	6.5

Table 4b Activation energies (kJ mol^{-1}) obtained from the non-linear regression for Arrhenius equation for MaterBi-Z and nanocomposites

Clay/mass%	MMT	C30B	C10A
0.0	8.4	8.4	8.4
0.5	8.2	7.9	6.7
1.0	7.2	6.6	6.5
2.5	8.6	8.3	8.4
5.0	9.3	8.7	8.9

matrix cause more heterogeneous nucleation, which is expected to obtain a lower E. But the addition of more layered silicate induced more steric hindrance and also reduces the transportation ability of polymer chains during crystallization processes (a higher E), the E increases as the content of layered silicate increases.

Figure 9 shows α experimental data and α values obtained with this model for MaterBi-Z and nanocomposites with 5 mass% of clay. α values calculated with Avrami model were in good agreement with experimental data. Similar results were obtained for different clay contents. It is possible to see that a higher crystallization temperature (lower undercooling) higher the crystallization time and lower the crystallization rate.

Conclusions

The isothermal crystallization of MaterBi-Z with different clay contents was studied. One of the most important effects of the layered silicate was related with the lower perfection of the crystallites: the more heterogeneous nucleation drove to a decrease on the theoretical melting temperature (T_m^0).

At low clay concentrations, the influence of silicate layers, as nucleating agents dominate, while at higher concentrations, the influence of silicate layers as growth retardants became more important because the diffusion of the polymer chains was hindered by the clay platelets.

Avrami model was able to predict the development of the crystallinity for all studied materials. Avrami exponent (n) values suggested that the matrix experienced a two dimensional crystal growth with a linear growth rate and the crystals nucleating athermally whereas in the case of nanocomposites the value was closer to 3, especially in the case of cloisite 10A indicating a spherical growth.

The Arrhenius type equation used for rate constant showed that the addition of layered silicate (0.5–1 mass%) into the matrix produced more heterogeneous nucleation whereas higher concentrations induced more steric hindrance reducing the transportation ability of polymer chains during crystallization processes.

Acknowledgements

Authors acknowledged to CONICET (PIP 6254) and ANPCyT.-Proyecto FONCyT-PICT N° 12-15074 and PICT 25766 for the financial support of this project.

References

1 C. Bastioli, The Wiley Encyclopedia of Packaging Technology, 2nd Ed., John Wiley & Sons Inc, 1987. p. 77.
2 C. Bastioli, Polym. Degrad. Stab., 59 (1998) 263
3 D. Plackett and A. Vázquez, Green Composites: Polymer Composites and the Environment, Chapter 5, Woodhead Publishers, C. Baillie, Ed., ISBN 1 85573 739, September, 2004.
4 V. P. Cyras, J. M. Kenny and A. Vázquez, Polym. Eng. Sci., 41 (2001) 1521.
5. V. P. Cyras, P. M. Stefani, R. A. Ruseckaite and A. Vázquez, Polym. Compos, 25 (2004) 461.
6 V. P. Cyras and A. Vázquez, 'Polímeros Biodegradables a Base de Almidón y Compuestos Biodegradables', Revista de Plásticos Modernos. ISSN 0034-8708, No 591, 2005 p. 223.
7 J. Xu, R. K. Y. Li, Y. Z. Heng and Y. W. Mai, Mater. Res. Bull., 41 (2006) 244.
8 P. Viville, R. Lazzaroni, E. Pollet, M. Alexandre, P. Dubois, G. Borcia and J. J. Pireaux, Langmuir, 19 (2003) 9425.
9 S. Ray and M. Okamoto, Prog. Polym. Sci., 28 (2003) 1539.
10 P. C. Le Baron, Z. Wang and T. J . Pinnavaia, Appl. Clay Sci., 15 (1999) 11.

11 X. Zheng and C. A. Wilkie, Polym. Degrad. Stab., 82 (2003) 441.
12 P. B. Messersmith and E. P. Giannelis, J. Polym. Sci. Part A: Polym. Chem., 33 (1995) 1047.
13 A. Usuki, T. Kawasumi, M. Kojima, Y. Fukushima and A. Okada, J. Mater. Res., 8 (1993) 1179.
14 Y. Kojima, A. Usuki, M Kawasumi, Y. Fukushima, A. Okada and T. Kurauchi, J. Mater. Res., 8 (1993) 1185.
15 Y. Di, S. Iannace, E. Di Maio and L. Nicolais, J. Polym. Sci. Part B: Polym. Phys., 41 (2003) 670.
16 Y. Di, S. Iannace, L. Sanguigno and L. Nicolais, Macromol. Symp., 228 (2005) 115
17 H. Fischer, Mater. Sci. Eng., C, 23 (2003) 763.
18 E. Di Maio, S. Iannace, L. Sorrentino and L. Nicolais, Polymer, 45 (2004) 8893.
19 T. D. Fornes and D. R. Paul, Polymer, 44 (2003) 3945.
20 M. Van Es, Polymer-clay Nanocomposites, Ph.D. Thesis, The Netherlands: Technical University of Delft. ISBN 90 77017 27 5; 2001 [chapter 7].
21 D. Homminga, B. Goderis, I. Dolbnya and G. Groeninckx, Polymer, 47 (2006) 1620.
22 K. E. Strawhecker and E. Manias, Chem. Mater, 15 (2003) 844.
23 M. Pluta, A. Galeski, M. Alexandre, M. A. Paul and P. Dubois, J. Appl. Polym. Sci., 86 (2002) 1497.
24 C. J. Pérez, V. A. Alvarez, P. M. Stefani and A. Vázquez, J. Therm. Anal. Cal, 88 (2007) 825.
25 C. C. Lin, Polym. Eng. Sci., 23 (1983) 113.
26 P. Cebe and S. D. Hong, Polymer, 27 (1986) 1183.
27 C. J. Pérez, V. A. Alvarez, I. Mondragón and A. Vázquez, Polym. Int., 56 (2007) 686.
28 S. Iannace and L. Nicolais, J. Appl. Polym. Sci., 64 (1997) 911.
29 P. Maiti and M. Okamoto, Macromol. Mater. Eng., 288 (2003) 440.
30 M. Avella, E. Martuscelli, C. Selliti and E. Garagnani, J. Mater. Sci., 22 (1987) 3185.
31 T. M. Wu and C. Y. Liu, Polymer, 46 (2005) 5621.
32 A. Janevsky and G. Bogoeva-Gaceva, J. Appl. Polym. Sci., 69 (1998) 381.
33 L. Torre, A. Maffezzoli and J. M. Kenny, J. Appl. Polym. Sci., 56 (1995) 985.
34 V. Krikorian and D. J. Pochan, Macromolecules, 37 (2004) 6480.
35 V. E. Reinsch and L. Rebenfeld, J. Appl. Polym. Sci., 52 (1994) 649.
36 G. P. Desio and L. Rebenfeld, J. Appl. Polym. Sci., 45 (1992) 2005.

Received: October 6, 2006
Accepted: January 18, 2007

DOI: 10.1007/s10973-007-8213-6